
ENSEMBLE LEARNING USING INDIVIDUAL NEONATAL DATA FOR SEIZURE DETECTION

Ana Borovac

Faculty of Industrial Engineering, Mechanical Engineering and Computer Science
 University of Iceland
 Kvikna Medical ehf.
 Reykjavik, Iceland
 anb48@hi.is

Steinn Gudmundsson

Faculty of Industrial Engineering, Mechanical Engineering and Computer Science
 University of Iceland
 Reykjavik, Iceland
 steinng@hi.is

Gardar Thorvardsson

Kvikna Medical ehf.
 Reykjavik, Iceland
 gardar@kvikna.com

Saeed M. Moghadam

BABA Center
 Helsinki University Hospital
 University of Helsinki
 Helsinki, Finland
 saeed.montazeri@helsinki.fi

Päivi Nevalainen

BABA Center
 Epilepsia Helsinki and Department of Clinical Neurophysiology
 Helsinki University Hospital
 University of Helsinki
 Helsinki, Finland
 paivi.nevalainen@hus.fi

Nathan Stevenson

Brain Modelling Group
 QIMR Berghofer Medical Research Institute
 Brisbane, Australia
 nathan.stevenson@QIMRBerghofer.edu.au

Sampsaa Vanhatalo

BABA Center
 Helsinki University Hospital
 University of Helsinki
 Helsinki, Finland
 sampsaa.vanhatalo@helsinki.fi

Thomas P. Runarsson

Faculty of Industrial Engineering, Mechanical Engineering and Computer Science
 University of Iceland
 Reykjavik, Iceland
 tpr@hi.is

ABSTRACT

Sharing medical data between institutions is difficult in practice due to data protection laws and official procedures within institutions. Therefore, most existing algorithms are trained on relatively small electroencephalogram (EEG) data sets which is likely to be detrimental to prediction accuracy. In this work, we simulate a case when the data can not be shared by splitting the publicly available data set into disjoint sets representing data in individual institutions. We propose to train a (local) detector in each institution and aggregate their individual predictions into one final prediction. Four aggregation schemes are compared, namely, the majority vote, the mean, the weighted mean and the Dawid-Skene method. The approach allows different detector architectures amongst the institutions.

The method was validated on an independent data set using only a subset of EEG channels. The ensemble reaches accuracy comparable to a single detector trained on all the data when sufficient amount of data is available in each institution. The weighted mean aggregation scheme showed best overall performance, it was only marginally outperformed by the Dawid-Skene method when local detectors approach performance of a single detector trained on all available data.

1 Introduction

Seizures are more common during perinatal period [13], and management of neonatal seizures requires timely detection and treatment to reduce ensuing brain damage [4]. The current gold standard for neonatal seizure detection is visual analysis by a human expert using a full-montage video electroencephalogram (EEG) [35]. Since such service is rarely available in neonatal intensive care units (NICUs), there is an urgent clinical need for automated neonatal seizure detection algorithm (NSDA) with human expert level accuracy.

Early automated NSDAs were based on *features*, quantitative descriptors of short, e.g. 10 – 16 sec long, EEG segments and expert-defined threshold decision rules [23, 26, 27]. Hard-coded thresholds were later replaced by statistical techniques, such as linear discriminant analysis [14], support vector machines (SVMs) [1, 3, 46] and neural networks [16]. Recently, promising results have been obtained using convolutional neural networks (CNNs) [2, 19, 30].

Deep neural networks (DNNs) generally require a large amount of training data [21]. However, building a large and diverse enough neonatal EEG data set with high quality seizure annotations is time consuming, ambiguous [24, 38] and often limited due to strict regulations (e.g. the Privacy Rule of the U.S. Health Insurance Portability and Accountability Act (HIPAA), or the European General Data Protection Regulation (GDPR)) making data sharing between institutions difficult, if not impossible [10, 54]. Challenges in sharing data have triggered growing interest in distributed approaches to statistical learning [20].

One approach that requires minimal sharing of information is model ensembling, i.e. models are trained locally at each institution and predictions on new data are aggregated (ensembled) from predictions made by the local models. This requires sharing only the models across the network of institutions rather than sharing the potentially sensitive, original biosignals. However, the procedures in model sharing need to be planned so that they mitigate the impact of possible inadvertent leaks of training data through a model [12, 56]. One solution to this problem is to have a *trusted agent* in charge of the models and an aggregation procedure. Compared to the federated learning [22], ensembling does not require communication between the institutions during the training phase (which may be difficult to set up) and it does not require the institutions to use the same model architecture. One institution could e.g. use a DNN, another an SVM and a third a decision tree classifier.

Once predictions on new data have been made there are a number of techniques by which they can be ensembled. If predictions are accompanied by probabilities they can be averaged [7, 50], if not, a commonly used method for label aggregation is to simply select the most frequent label, referred to as *majority vote* in the following. One could also put more weight on some predictions if they are *a priori* more trustworthy, otherwise, an estimate of each annotator performance can be used [43, 48, 52]. In 1979 Dawid and Skene [8] used an expected maximization (EM) algorithm [9] to estimate annotator performance and provide consensus labels.

Ensemble learning has previously been used in neonatal seizure detection. In [32] stacking is used where different model types trained on the same data are combined. In [42] three identical NSDAs are trained on the same EEG data but using labels from different experts. In this work we use ensemble learning on disjoint data sets, to simulate the situation where institutions train NSDAs on locally available data. Our aim is to investigate the necessity of sharing data in order to approach the state-of-the-art performance of an automated NSDA. For aggregation we compared the majority vote, the mean, the weighted mean (via stacking) and the Dawid–Skene expected maximization algorithm. We show that the weighted mean outperforms the other methods if the NSDAs in the ensemble are trained on a very few patients and Dawid-Skene marginally outperforms the other methods when the local NSDAs are not much worse than a baseline NSDA. In these cases the aggregated predictions also reach performance of the baseline NSDA performance.

2 Methods

Multiple local models, referred to as *local NSDAs* in the following, are trained on disjoint subsets of multi-channel EEG recordings, simulating a scenario where several hospitals train NSDAs individually, without sharing patient data. The trained detectors are then shared with a trusted agent. To classify a short EEG segment from a new patient as seizure/non-seizure, the trusted agent sends the segment through all the local NSDAs and the predictions are aggregated.

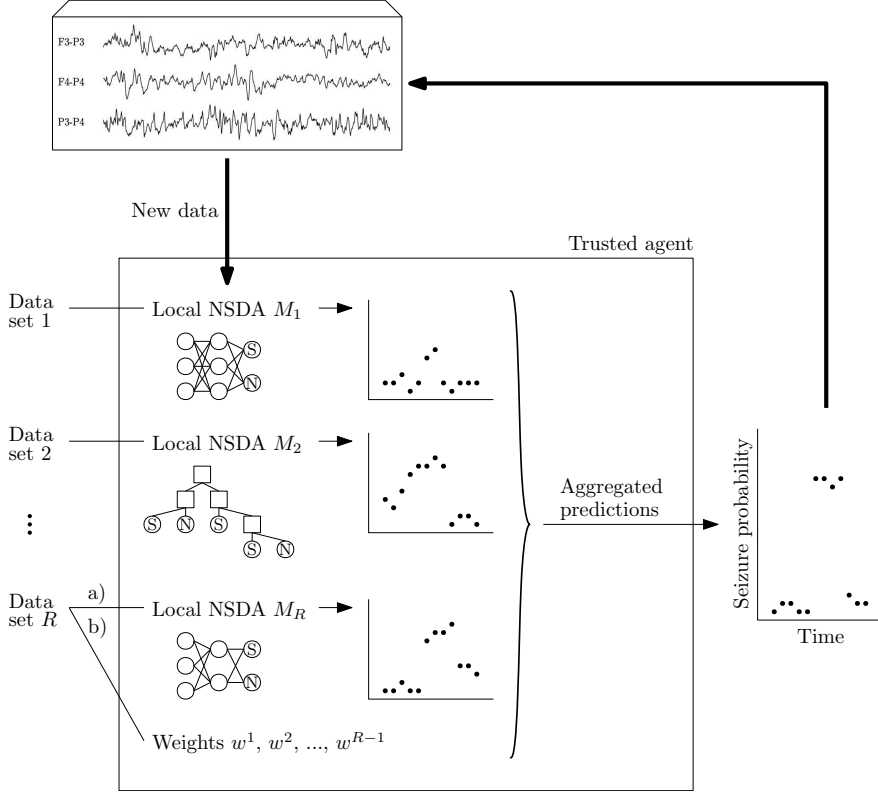


Figure 1: A schematic diagram of the proposed method. Each data set is used to train a local NSDAs or weights that are shared with a trusted agent. The trusted agent makes predictions on new data. Seizure predictions for new data are obtained a) by aggregating predictions made by R NSDAs using the majority vote, the mean or the Dawid–Skene method, or, b) by aggregating predictions made by $R - 1$ local NSDAs using the weighted mean (weights are learned on the R^{th} data set).

gated using one of the following schemes: majority vote, mean, weighted mean or the Dawid–Skene method. The methodology is summarized in figure 1.

For local NSDAs, we used DNNs which take EEG segments as input, however any other type of NSDA could be used as well. The networks share the same architecture but have different network weights since they were trained on disjoint training sets.

2.1 Aggregation methods

In the following we consider a binary classification problem where the classes are labeled 0 and 1. Let D be a set of N predictions from R independent models

$$D = \{(p_1^1, p_1^2, \dots, p_1^R), \dots, (p_N^1, p_N^2, \dots, p_N^R)\},$$

where p_i^j is the estimated probability of model j of instance i belonging to class 1. By setting a threshold between the classes to 0.5, the predicted label of model j of instance i is given by

$$y_i^j = \begin{cases} 1; & \text{if } p_i^j \geq 0.5 \\ 0; & \text{otherwise} \end{cases}.$$

A simple way to aggregate multiple predictions for instance i , when models do not output their confidence (e.g. class probabilities), is to use majority vote, i.e. select the most frequent label. Here we use the mean of predicted labels,

$$\mu_i^{MV} = \frac{1}{R} \sum_{j=1}^R y_i^j; \quad i \in \{1, 2, \dots, N\}. \quad (1)$$

When the models output class probabilities, which is e.g. the case when the models correspond to the neural networks, the predictions can be aggregated by taking the mean probability

$$\mu_i^M = \frac{1}{R} \sum_{j=1}^R p_i^j; \quad i \in \{1, 2, \dots, N\}. \quad (2)$$

As some of the models might perform better than others, a weighted mean can be used to emphasize the more accurate models. To get the final prediction in a range between 0 and 1, we used logistic regression

$$\mu_i^{WM} = \sigma \left(\sum_{j=1}^R w^j p_i^j \right); \quad i \in \{1, 2, \dots, N\}, \quad (3)$$

where $\sigma(x) = 1/(1+e^{-x})$. The weights for w^j are learned on a held out data set (see section 2.4).

The fourth aggregation method evaluated here is the Dawid–Skene method. The method estimates the sensitivity and specificity of each model, together with consensus predictions μ^{DS} . For details of the method see appendix A.

2.2 Data

The EEG data used to train the NSDAs is a publicly available data set containing 79 approximately one hour long neonatal EEG recordings, measured with 19 Ag/AgCl electrodes positioned according to the 10-20 system [40]. An 18 channel montage was used, i.e. we derived channels Fp2-F4, F4-C4, C4-P4, P4-O2, Fp1-F3, F3-C3, C3-P3, P3-O1, Fp2-F8, F8-T4, T4-T6, T6-O2, Fp1-F7, F7-T3, T3-T5, T5-O1, Fz-Cz and Cz-Pz. The recordings were annotated by three EEG experts where each second in a recording is annotated as a seizure or non-seizure. We refer to this data set as 18-channel DS below.

The second, proprietary, data set (3-channel DS) consisting of EEG recordings of 28 neonates, was used as a held out test set to evaluate the aggregation schemes in a real world setting, i.e. detectors were trained on 18-channel DS and tested on this data set. The data set is also used in [44] and is a subset of the data set used in [28]. Institutional Research Review Board of the HUS diagnostic center approved the use of this data, including a waiver of consent due to the study's retrospective and observational nature. Each recording spans from 19 hours to 7 days. The recordings were obtained using 4 needle electrodes (F3, F4, P3 and P4) with a common reference, instead of the full set of 19 electrodes used in the training data set. Neonatal recordings are typically performed with this reduced electrode set to allow easier maintenance in a long duration brain monitoring [6]. The three bipolar derivations (F3-P3, F4-P4 and P3-P4) were used for both two human expert annotations and as the detectors input.

Additional attributes of the data sets are given in appendix B.

Each EEG recording was cut into 16 sec long segments with 12 sec overlap. Out of the 79 (28) recordings in 18-channel DS (3-channel DS), 38 (24) contain at least one seizure longer than 16 sec identified by three (two) human experts, meaning each of these recordings contain at least one consensus seizure segment. Segments containing more than 1 sec of zero voltage interval in at least one channel (disconnected electrode or pause in the recording) were left-out from the training and test sets. The signals were filtered with a 6th order Chebyshev Type 2 band-pass filter with cut-off frequencies of 0.5 Hz and 16 Hz, down-sampled to 32 Hz and rescaled to 16-bit integers. This is similar to the pre-processing in [46, 19].

2.3 Neonatal seizure detection algorithm

Each NSDA is a neural network consisting of three components; a feature extractor, an attention layer and an output layer. The feature extractor is a CNN from [29]. The features are extracted from each EEG channel separately and are combined into a single feature channel by the attention layer [19]. The attention layer is used since expert labels are not specific to individual channels and neonatal seizures tend to be partial [35], i.e. localized in a small area of the brain and therefore only present in a subset of the recorded channels. The attention layer is also independent of the number of input feature channels making the detector independent of the number of recorded EEG channels. The output layer is a fully connected layer with two output nodes representing the two classes. A detailed description of the network architecture is given in appendix C.

To compare the aggregation methods to current state-of-the-art NSDAs, we trained a neural network using all the recordings in 18-channel DS containing at least one consensus seizure longer than 16 sec (P). This NSDA is referred to as the *baseline NSDA* in the following.

The local NSDAs use the same neural network architecture as the baseline NSDA but differ in the data used for training. The patients in P (patients containing a consensus seizure) were partitioned into k subsets representing data sets in individual institutions. Partitioning was random such that each patient was in exactly one subset and there were at least 3 patients in every subset. The union of the k subsets was then P , the data set used as a training set for the baseline NSDA. By excluding patients without consensus seizures we ensured each subset had patients with seizures and eliminated the varying number of EEG with normal brain activity in individual subsets making the analysis more straightforward. As there can be a big difference between the training set sizes, we obtained local NSDAs with different generalisation strengths and consequently with different performance strengths on an unseen data. This is expected in practice. Depending on the patient cohorts, recording set-ups and other factors the detectors will perform differently on an unseen data. The value of k ranged from 3 to 10.

2.4 Training

After partitioning the training set, each NSDA (baseline NSDA and local NSDAs) was trained on 16 sec long EEG segments corresponding to the consensus seizures and an equal number of randomly chosen non-seizure segments. Segments with disagreements between the human experts and partly seizure/non-seizure segments were not included in the training sets. Cross entropy was used as the loss function. The Adam optimizer was used to optimize the network weights using an initial learning rate of 0.001 which was then halved every 10 epochs. The NSDAs were trained for 30 epochs with a mini-batch size of 32. Hyper-parameters, learning rate and number of epochs, were tuned empirically, from observing the behavior of the loss function during the training of the baseline NSDA. A small mini-batch size was chosen due to a small amount of data used in some local NSDAs.

For the weighed mean aggregation scheme, the weights w^j , $j \in \{1, 2, \dots, R\}$, were learned using a stacking classifier [52]. A logistic regression classifier was trained using the data from one randomly selected local NSDA in each experiment. This local NSDA was not used in an ensemble for making predictions on a test patient. Therefore, non-overlapping data sets were used for training the local NSDAs and the logistic regression classifier. Also, the training data of the local NSDAs would not need to be shared in practice as the input of the logistic regression classifier is just a set of seizure probabilities estimated by the local NSDAs and these can be provided by the trusted agent.

All the deep learning code used in the experiments was implemented using PyTorch 1.7.1 [33] and run on an NVIDIA GTX 1080 Ti GPU. For logistic regression, we used the scikit-learn [34] implementation with default hyper-parameters. The code is available at github.com/anaborovac/Distributed-NSDA (currently inactive link).

2.5 Performance

To avoid overlap between training and test data when evaluating classifier performance on the 18-channel DS, leave-one-subject-out cross-validation was used. This entailed training 38 baseline NSDAs, 38 sets of local NSDAs and 38 sets of logistic regression classifiers, leaving out data from one subject (patient) at a time. The experiment was repeated 10 times, resulting in $10 \cdot 38 \cdot (3+4+\dots+10) = 19760$ local NSDAs and $10 \cdot 38 \cdot (1+1+\dots+1) = 10 \cdot 38 \cdot 8 = 3040$ logistic regression classifiers.

Data from each left-out patient was sent through the corresponding baseline NSDA and local NSDAs. Predictions from the baseline NSDAs were compared to human expert labels to obtain performance metrics. Predictions from the local NSDAs were first aggregated using one of the aforementioned aggregation schemes: majority vote (1), mean (2), weighted mean (3) and the Dawid–Skene method (appendix A) to obtain the final predictions and these were then compared to human expert labels.

Two sets of performance metrics were calculated, metrics based on the success/failure in classifying individual 16 sec long segments, and event-based metrics which indicate whether a seizure was detected at all, or whether a seizure was falsely reported. The segment-based metrics are sensitivity (SE), specificity (SP) and the area under the receiver operating characteristic curve (AUC). These metrics were calculated from segments without disagreements between human experts and segments with either seizure either non-seizure activity for the whole segment duration. The event-based metrics are seizure detection rate (SDR), false detections per hour (FD/h) and the mean false detection duration (MFDD) [47]. A consensus seizure was considered to be detected if it was detected at any point in time and a seizure was considered as a false detection if it did not overlap with any (consensus or not) seizure labelled by the human experts. Definitions of the metrics are provided in appendix D. Metrics calculated on each patient separately were summarized by their means and medians.

Before the event-based metrics were calculated a post-processing step was in order since segments overlap. Besides a few segments at the beginning and end of each recording, for each 4 sec long segment there are 4 overlapping 16 sec long segments. Prediction for a 4 sec segment was obtained by averaging predictions from overlapping 16 sec long

Table 1: Accuracy of the baseline model. Area under the curve (AUC), sensitivity (SE), specificity (SP), seizure detection rate (SDR), false detections per hour (FD/h) and mean false detection duration (MFDD) are computed as the mean and median over all the patients with seizures.

		Segment-based metrics		
		AUC	SE [%]	SP [%]
18-channel DS	median	0.98	90	97
	mean	0.92	80	94
18-channel ₃ DS	median	0.94	78	99
	mean	0.88	67	98
3-channel DS	median	0.93	78	98
	mean	0.92	71	97
Event-based metrics				
		SDR [%]	FD/h	MFDD [s]
18-channel DS	median	100	0.91	12.0
	mean	85	1.99	19.15
18-channel ₃ DS	median	100	0.0	0.0
	mean	76	0.78	8.98
3-channel DS	median	96	0.97	15.82
	mean	90	1.37	17.92

segments [18, 31]. Seizures with duration less than 10 sec were excluded and considered normal brain activity as by definition seizures are longer than 10 sec [49].

For studying the segment-based level of agreement between the local NSDAs we used Gwet’s first-order agreement coefficient (AC1) [15]. Compared to the often used Cohen’s (Fleiss’) κ [19, 5, 41], Gwet’s AC1 is less prone to the paradoxes associated with highly imbalanced data [11, 53].

Performance on 3-channel DS was evaluated in the same manner as for 18-channel DS, i.e. the metrics were calculated for each patient separately and then summarized with the mean and the median. The baseline NSDA was trained using all 38 patients in P (no patients were left-out), and the union of the training sets for the local NSDAs also contained all 38 patients in P . This resulted in additional $1+10 \cdot (3+4+\dots+10) = 521$ NSDAs and $10 \cdot (1+1+\dots+1) = 10 \cdot 8 = 80$ logistic regression classifiers.

3 Results

To assess the clinical usefulness of the aggregation schemes they are compared to a baseline NSDA which is trained on data from all 38 patients in P (in a leave-one-subject-out setting for evaluation on 18-channel DS). The baseline NSDA thus corresponds to the situation where a single agent has access to all the training data (P), a situation which is expected to be favorable compared to aggregating predictions from multiple models trained on subsets of the same data.

3.1 Baseline NSDA

Table 1 shows the performance of the baseline detector trained on 18-channel DS and tested with leave-one-subject-out on 18-channel DS, as well as the results of testing the detector on the held out 3-channel DS. We also included results on 18-channel DS when the inputs were limited to the 3 channels used in 3-channel DS (18-channel₃ DS). For this analysis the NSDAs did not need to be re-trained as they are independent of the number of input channels. It is worth noting that the performance estimates for the baseline NSDA are clearly affected by whether the mean or the median is used as a summary statistic for the chosen metric indicating an asymmetry in distribution of performance measures.

The performance on 18-channel DS was in line with previous studies which also used 18-channel DS; Stevenson et al. [41] reported a median AUC of 0.99 (leave-one-subject-out testing), O’Shea et al. [30] reported a mean AUC of 0.96 (trained on a proprietary data set) and Isaev et al. [19] obtained a mean AUC of 0.92 (trained on a proprietary

data set). The performance of an NSDA on an independent test set is usually worse than performance estimates obtained from a held out training data. Such a decrease can be attributed to several factors, including differences in patient cohorts, recording equipment, seizure prevalence, the number of available EEG channels, the human experts that annotated the EEG [5], and training data not representing the general population. For example, the mean AUC decreased from 0.97 to 0.92 in [19] and from 0.99 to 0.96 in [30]. We observed a similar drop in performance when the baseline detector was tested on 3-channel DS. The AUC and specificity were only slightly affected, but the sensitivity was about 10 % lower than for 18-channel DS. This can partly be explained by the small number of EEG channels available in 3-channel DS (3 vs. 18 in the training data) and consequently the optimal detection threshold between the classes (seizure/non-seizure) may be different. We confirmed this finding by testing the base classifier on 18-channel₃ DS. In this case, some of the missed seizures might simply be due to seizure activity not being present in any of the three channels used in 18-channel₃ DS [37, 39, 45], whereas the annotators had access to all 18 channels. Reducing the number of channels also led to a removal of some seizure-like patterns [51], such as respiratory and heart rate artefacts, resulting in a low false detection rate on 18-channel₃ DS. An example is given in appendix E.

The event-based metrics showed similar behavior across the data sets (18-channel DS and 3-channel DS). A decrease in sensitivity while the seizure detection ratio is barely affected on 3-channel DS indicates that some seizures are only partly detected. As uncertainty in seizure onset and offset is higher when a reduced montage is used, human experts tend to annotate longer seizures to ensure annotation spans through the whole seizure. This intervals of uncertainty may not be detected by the automatic detector.

In summary, the baseline NSDA gives comparable results to the state-of-the-art NSDAs and performs well on recordings which include only a small subset of the channels used in training.

3.2 Local NSDAs

Before comparing the different aggregation schemes, we analyzed the performance of individual local NSDA, to study how the performance is affected by the number of patients available for training. When a larger number of local NSDAs is used, the number of patients in an individual training set decreases since the total number of patients in the training sets is constant (37 for 18-channel DS and 38 for 3-channel DS). We quantify this behaviour with the mean median number of patients in the training set. E.g. if 4 local NSDAs are used and the mean median is 8.1, then on average there are at least 9 patients in the training of 2 of the local NSDAs.

The results for local NSDAs trained on data from approx. 3 to approx. 11 patients and tested on a left-out patient from 18-channel data set and individual patient from 3-channel data set is shown in figure 2. As expected, when data from more patients was included in each NSDA, the detectors became more accurate, the area under the curve and the seizure detection rate increased, and the false detection rate decreased. All measures approached the corresponding values for the baseline NSDA. Conversely, the values of all performance metrics degraded when most of the local NSDAs were trained on a small number of patients. This is unsurprising since a small training data is not likely to be a good representation of the entire population. We also observed a low agreement between the NSDAs trained on just a few patients (appendix E).

Figure 2 also shows that for any number of local NSDAs there are some detectors with poor performance. They may be trained on a small data set, or, they are one of the few recordings which appears to be quite difficult to classify correctly even for the baseline NSDA, for reasons that are not entirely clear.

3.3 Aggregation methods

Here we evaluate the different aggregation schemes and compare them to the baseline NSDA and to the average performance of the local NSDAs. If the baseline performance can be reached with an aggregation scheme, it would indicate that the data does not need to be shared during the training of a NSDA to obtain a detector with state-of-the-art performance. The four aggregation schemes majority vote, mean, weighted mean and Dawid–Skene were evaluated on 18-channel DS and 3-channel DS for $k = 3, 4, \dots, 10$ local NSDAs. Results for the majority vote are not shown since in all cases majority vote was slightly outperformed by the mean aggregation scheme (see appendix E).

Figure 3 shows area under the curve is comparable between all aggregation schemes and to the baseline NSDA. However, differences in seizure detection rate and false detections per hour are spotted.

The seizure detection rate behaves similarly for both data sets. For the Dawid–Skene method the values are comparable to the baseline NSDA, for all k tested, while for the mean and the weighted mean aggregation schemes the values decrease with an increased number of local NSDAs. Recall that when there are few NSDAs, each NSDA contains a large number of patients on average, and vice versa. The mean aggregation scheme performed slightly worse than the weighted mean and both performed notably worse than Dawid–Skene for $k \geq 4$. Moreover, for 18-channel DS the

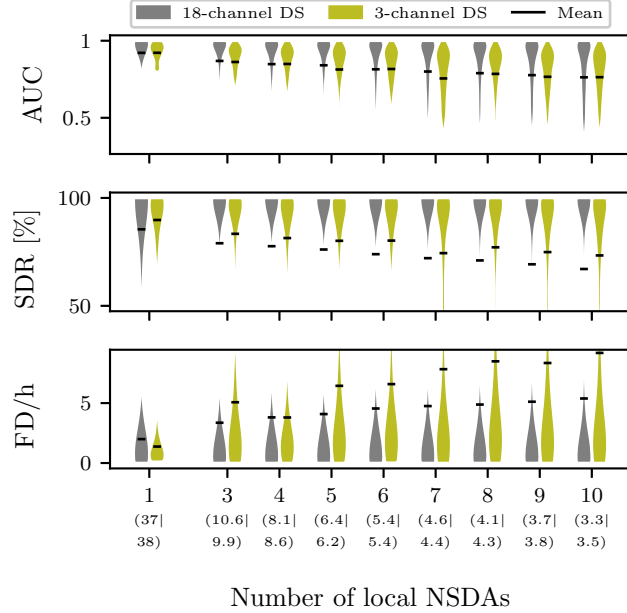


Figure 2: Performance of individual local NSDAs. Area under the curve (AUC), seizure detection rate (SDR) and false detections per hour (FD/h) of the local NSDAs as a function of the number of local NSDAs. The average (across ten runs) mean median number of patients in each NSDA is shown in parentheses. Each local NSDA was tested on a left-out patient from 18-channel DS or 3-channel DS.

average seizure detection rate of the local NSDAs is comparable to the values corresponding to the mean aggregation scheme, for 3-channel DS the mean aggregation scheme marginally outperformed the average seizure detection rate of the local NSDA for $k \geq 7$. The weighted mean outperforms the mean aggregation scheme for $k \geq 8$ ($k = 10$) on 18-channel DS (3-channel DS), for smaller k the mean and the weighted mean aggregation schemes return comparable seizure detection rates.

Moreover, in figure 3 we observe that the average false detections per hour of the local NSDAs is outperformed by all aggregation schemes. The average false detections per hour of the local NSDAs are noticeably higher for 3-channel DS than for 18-channel DS, in particular for $k \geq 6$. One possible explanation is that the recordings in 3-channel DS are much longer and on average just 3.5 % of a recording corresponds to a seizure activity. The mean aggregation scheme behaves similarly on both data sets, the values are lower than for the baseline NSDA and the measure decreases with increasing k . This may be a result of low level of agreement between the local NSDAs for the large k . So, even though an individual local NSDA falsely detects a large number of seizures, the aggregated prediction filters out the misclassified non-seizure segments due to low agreement between the local NSDAs. This may on the other hand caused problems with the Dawid-Skene method, i.e. the false detections per hour increased slowly on 18-channel DS and rapidly on 3-channel DS with increasing k . In contrast, the logistic regression classifier determining the weights for the weighted mean aggregation scheme successfully detected local NSDAs with low false detection rate for all k tested.

We observed low false detection rates for the mean and weighted mean aggregation schemes and therefore investigated whether the false detections are short or long in duration. We did not observe big differences between the aggregation schemes and different values of local NSDAs (figure 8 in appendix E).

To summarise, all aggregation schemes tested here performed better than the average local NSDA and were comparable to the baseline NSDA for $k \in \{3, 4\}$. Poorer performances for the larger k values are mainly a result of training the local NSDAs on smaller training sets not capturing the general population. The (weighted) mean aggregation scheme does not detect as many seizures as the baseline model, however the false detection per hour is comparable if not lower. The Dawid-Skene method successfully detects the same number of seizures as the baseline NSDA for any k , but the false detection is compromised for $k \geq 6$. Predictions obtained with the Dawid-Skene are difficult to explain [17, 55], only a few local NSDAs with poor performance may have caused unexpected and undesired aggregated prediction [25]. For a large number ($k \geq 6$) of local NSDAs the logistic regression classifier estimated performances of local NSDAs

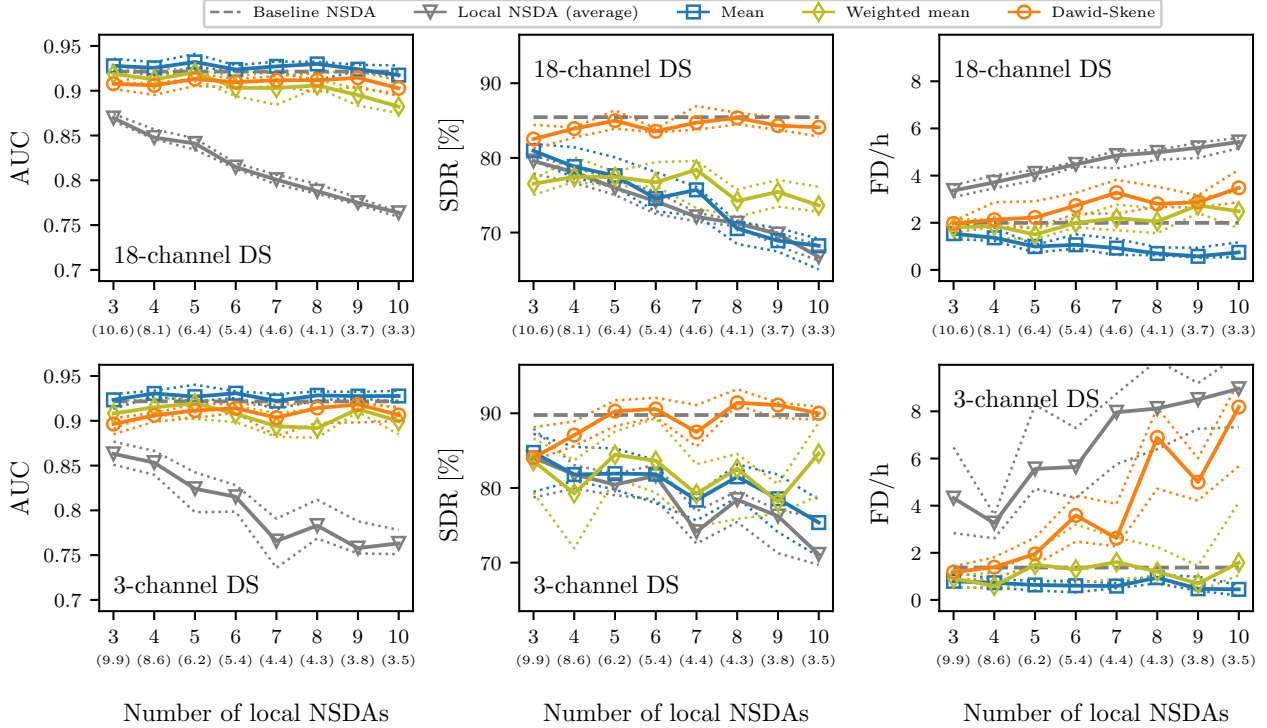


Figure 3: Average area under the curve (AUC), seizure detection rate (SDR) and false detections per hour (FD/h) as a function of the number of local NSDAs used in the aggregation schemes. The solid lines represent the medians of ten runs and dotted lines represent the corresponding inter-quartile ranges. The grey dashed line represents the average metric of the baseline NSDA. The average (across ten runs) mean median number of patients in each NSDA is shown in parentheses.

better than the Dawid-Skene, i.e. the aggregated predictions did not contain a large number of falsely detected seizures and low seizure detection rate.

4 Conclusion

In this work we have shown that an NSDA based on a convolutional neural network together with an attention layer can accurately detect seizures, even if the data is obtained with different types of electrodes (scalp vs needle) and significantly lower number of channels than it was used for training. Channel reduction also caused removal of some artefacts with seizure-like patterns as the region around F3, F4, P3 and P4 electrodes is less prone to the artefacts, resulting in an unforeseen low false detection rate.

All performance metrics of NSDAs unsurprisingly dropped when training sets contained data from only a few patients. For aggregation of such NSDAs the weighted mean aggregation scheme performed best. Compared to the Dawid-Skene method, it successfully detected local NSDAs with high false detection rates and seizure detection rate was not as compromised as it was for the mean aggregation scheme. When a larger number of patients was included in the training of individual local NSDAs, i.e. when the number of local NSDAs was few, the Dawid-Skene marginally outperformed the other aggregation schemes. It returned higher seizure detection rate and the false detections per hour was comparable to the (weighted) mean aggregation scheme. Independent of the number of local NSDAs, the majority vote was just slightly outperformed by the mean aggregation scheme and all aggregation schemes performed better than the average individual performance.

Based on the performed experiments the weighted mean aggregation scheme showed best overall performance and was comparable to the state-of-the-art of an automatic NSDA when a larger number of patients were included in the training of an individual local NSDA. This indicates that data does not need to be shared between institutions as long as there is a fair amount of data available in each institution. To confirm these simulation based findings in a real-world setting, data from multiple institutions would be required. It would also be interesting to include ECG and respiratory

signals (when available) in the detection process to potentially reduce false detections associated with these biological artefacts.

Acknowledgment

This project receives funding from the Sigrid Juselius Foundation and the European Union’s Horizon 2020 research and innovation programme under grant agreement No 813483.

References

- [1] Rehan Ahmed, Andriy Temko, William P Marnane, Geraldine B Boylan, and Gordon Lightbody. Exploring temporal information in neonatal seizures using a dynamic time warping based SVM kernel. *Computers in biology and medicine*, 82:100–110, 2017.
- [2] Amir H Ansari, Perumpillichira J Cherian, Alexander Caicedo, Gunnar Naulaers, Maarten de Vos, and Sabine Van Huffel. Neonatal seizure detection using deep convolutional neural networks. *International journal of neural systems*, 29(04):1850011, 2019.
- [3] Amir H Ansari, PJ Cherian, Anneleen Dereymaeker, Vladimir Matic, Katrien Jansen, Leen de Wispelaere, C Dielman, J Vervisch, Renate Swarte, Paul Govaert, et al. Improved multi-stage neonatal seizure detection using a heuristic classifier and a data-driven post-processor. *Clinical Neurophysiology*, 127(9):3014–3024, 2016.
- [4] Stella T Björkman, Stephanie M Miller, Stephen E Rose, Christopher Burke, and Paul B Colditz. Seizures are associated with brain injury severity in a neonatal model of hypoxia–ischemia. *Neuroscience*, 166(1):157–167, 2010.
- [5] Ana Borovac, Steinn Gudmundsson, Gardar Thorvardsson, and Thomas P Runarsson. Influence of human-expert labels on a neonatal seizure detector based on a convolutional neural network. In *The NeurIPS 2021 Data-Centric AI Workshop*, December 2021.
- [6] Geraldine B Boylan, Nathan J Stevenson, and Sampsaa Vanhatalo. Monitoring neonatal seizures. In *Seminars in Fetal and Neonatal Medicine*, volume 18, pages 202–208. Elsevier, 2013.
- [7] Ken Chang, Niranjan Balachandar, Carson Lam, Darvin Yi, James Brown, Andrew Beers, Bruce Rosen, Daniel L Rubin, and Jayashree Kalpathy-Cramer. Distributed deep learning networks among institutions for medical imaging. *Journal of the American Medical Informatics Association*, 25(8):945–954, 2018.
- [8] Alexander Philip Dawid and Allan M Skene. Maximum likelihood estimation of observer error-rates using the EM algorithm. *Journal of the Royal Statistical Society: Series C (Applied Statistics)*, 28(1):20–28, 1979.
- [9] Arthur P Dempster, Nan M Laird, and Donald B Rubin. Maximum likelihood from incomplete data via the EM algorithm. *Journal of the Royal Statistical Society: Series B (Methodological)*, 39(1):1–22, 1977.
- [10] Johanna Eicher, Raffael Bild, Helmut Spengler, Klaus A Kuhn, and Fabian Prasser. A comprehensive tool for creating and evaluating privacy-preserving biomedical prediction models. *BMC Medical Informatics and Decision Making*, 20(1):1–14, 2020.
- [11] Alvan R Feinstein and Domenic V Cicchetti. High agreement but low kappa: I. The problems of two paradoxes. *Journal of clinical epidemiology*, 43(6):543–549, 1990.
- [12] Matt Fredrikson, Somesh Jha, and Thomas Ristenpart. Model inversion attacks that exploit confidence information and basic countermeasures. In *Proceedings of the 22nd ACM SIGSAC conference on computer and communications security*, pages 1322–1333, 2015.
- [13] Hannah C Glass, Courtney J Wusthoff, Renée A Shellhaas, Tammy N Tsuchida, Sonia Lomeli Bonifacio, Malaika Cordeiro, Joseph Sullivan, Nicholas S Abend, and Taeun Chang. Risk factors for EEG seizures in neonates treated with hypothermia: a multicenter cohort study. *Neurology*, 82(14):1239–1244, 2014.
- [14] Barry R Greene, Stephen Faul, William Marnane, Gordon Lightbody, Irina Korotchikova, and Geraldine B Boylan. A comparison of quantitative EEG features for neonatal seizure detection. *Clinical Neurophysiology*, 119(6):1248–1261, 2008.
- [15] Kilem L Gwet. *Handbook of inter-rater reliability: The definitive guide to measuring the extent of agreement among raters*. Advanced Analytics, LLC, 2014.
- [16] Hamid Hassanzpour, Mostefa Mesbah, and Boualem Boashash. Time–frequency based newborn EEG seizure detection using low and high frequency signatures. *Physiological Measurement*, 25(4):935, 2004.

[17] Shahana Ibrahim, Xiao Fu, Nikolaos Kargas, and Kejun Huang. Crowdsourcing via pairwise co-occurrences: Identifiability and algorithms. *Advances in neural information processing systems*, 32, 2019.

[18] Thorir Mar Ingolfsson, Andrea Cossettini, Xiaying Wang, Enrico Tabanelli, Giuseppe Tagliavini, Philippe Ryvlin, and Luca Benini. Towards Long-term Non-invasive Monitoring for Epilepsy via Wearable EEG Devices. *arXiv preprint arXiv:2106.08008*, 2021.

[19] Dmitry Yu Isaev, Dmitry Tchapyjnikov, C Michael Cotten, David Tanaka, Natalia Martinez, Martin Bertran, Guillermo Sapiro, and David Carlson. Attention-based network for weak labels in neonatal seizure detection. *Proceedings of machine learning research*, 126:479, 2020.

[20] Margarita Kirienko, Martina Sollini, Gaia Ninatti, Daniele Loiacono, Edoardo Giacomello, Noemi Gozzi, Francesco Amigoni, Luca Mainardi, Pier Luca Lanzi, and Arturo Chiti. Distributed learning: a reliable privacy-preserving strategy to change multicenter collaborations using AI. *European Journal of Nuclear Medicine and Molecular Imaging*, pages 1–14, 2021.

[21] Yann LeCun, Yoshua Bengio, and Geoffrey Hinton. Deep learning. *Nature*, 521(7553):436–444, 2015.

[22] Tian Li, Anit Kumar Sahu, Ameet Talwalkar, and Virginia Smith. Federated learning: Challenges, methods, and future directions. *IEEE Signal Processing Magazine*, 37(3):50–60, 2020.

[23] A Liu, JS Hahn, GP Heldt, and RW Coen. Detection of neonatal seizures through computerized EEG analysis. *Electroencephalography and clinical neurophysiology*, 82(1):30–37, 1992.

[24] Aileen Malone, C Anthony Ryan, Anthony Fitzgerald, Louise Burgoyne, Sean Connolly, and Geraldine B Boylan. Interobserver agreement in neonatal seizure identification. *Epilepsia*, 50(9):2097–2101, 2009.

[25] Chenglin Miao, Qi Li, Lu Su, Mengdi Huai, Wenjun Jiang, and Jing Gao. Attack under disguise: An intelligent data poisoning attack mechanism in crowdsourcing. In *Proceedings of the 2018 World Wide Web Conference*, pages 13–22, 2018.

[26] Soundharya Nagasubramanian, Banu Onaral, and Robert Clancy. On-line neonatal seizure detection based on multi-scale analysis of EEG using wavelets as a tool. In *Proceedings of the 19th Annual International Conference of the IEEE Engineering in Medicine and Biology Society.'Magnificent Milestones and Emerging Opportunities in Medical Engineering'(Cat. No. 97CH36136)*, volume 3, pages 1289–1292. IEEE, 1997.

[27] Michael A Navakatikyan, Paul B Colditz, Chris J Burke, Terrie E Inder, Jane Richmond, and Christopher E Williams. Seizure detection algorithm for neonates based on wave-sequence analysis. *Clinical Neurophysiology*, 117(6):1190–1203, 2006.

[28] Päivi Nevalainen, Marjo Metsäranta, Sanna Toivainen-Salo, Tuula Lönnqvist, Sampsa Vanhatalo, and Leena Lauronen. Bedside neurophysiological tests can identify neonates with stroke leading to cerebral palsy. *Clinical Neurophysiology*, 130(5):759–766, 2019.

[29] Alison O’Shea, Gordon Lightbody, Geraldine Boylan, and Andriy Temko. Investigating the impact of CNN depth on neonatal seizure detection performance. In *2018 40th Annual International Conference of the IEEE Engineering in Medicine and Biology Society (EMBC)*, pages 5862–5865. IEEE, 2018.

[30] Alison O’Shea, Gordon Lightbody, Geraldine Boylan, and Andriy Temko. Neonatal seizure detection from raw multi-channel EEG using a fully convolutional architecture. *Neural Networks*, 123:12–25, 2020.

[31] Una Pale, Tomas Teijeiro, and David Atienza. Systematic assessment of hyperdimensional computing for epileptic seizure detection. *arXiv preprint arXiv:2105.00934*, 2021.

[32] Yini Pan, Hongfeng Li, Lili Liu, Quanzheng Li, Xinlin Hou, and Bin Dong. aEEG Signal Analysis with Ensemble Learning for Newborn Seizure Detection. In *International Workshop on Multiscale Multimodal Medical Imaging*, pages 76–84. Springer, 2019.

[33] Adam Paszke, Sam Gross, Francisco Massa, Adam Lerer, James Bradbury, Gregory Chanan, Trevor Killeen, Zeming Lin, Natalia Gimelshein, Luca Antiga, Alban Desmaison, Andreas Kopf, Edward Yang, Zachary DeVito, Martin Raison, Alykhan Tejani, Sasank Chilamkurthy, Benoit Steiner, Lu Fang, Junjie Bai, and Soumith Chintala. PyTorch: An Imperative Style, High-Performance Deep Learning Library. In H. Wallach, H. Larochelle, A. Beygelzimer, F. d’Alché-Buc, E. Fox, and R. Garnett, editors, *Advances in Neural Information Processing Systems 32*, pages 8024–8035. Curran Associates, Inc., 2019.

[34] Fabian Pedregosa, Gaël Varoquaux, Alexandre Gramfort, Vincent Michel, Bertrand Thirion, Olivier Grisel, Mathieu Blondel, Peter Prettenhofer, Ron Weiss, Vincent Dubourg, et al. Scikit-learn: Machine learning in Python. *Journal of machine learning research*, 12(Oct):2825–2830, 2011.

[35] Ronit M Pressler, Maria Roberta Cilio, Eli M Mizrahi, Solomon L Moshé, Magda L Nunes, Perrine Plouin, Sampsaa Vanhatalo, Elissa Yozawitz, Linda S de Vries, Kollencheri Puthenveettil Vinayan, et al. The ILAE classification of seizures and the epilepsies: Modification for seizures in the neonate. Position paper by the ILAE Task Force on Neonatal Seizures. *Epilepsia*, 62(3):615–628, 2021.

[36] Vikas C Raykar, Shipeng Yu, Linda H Zhao, Gerardo Hermosillo Valadez, Charles Florin, Luca Bogoni, and Linda Moy. Learning from crowds. *Journal of Machine Learning Research*, 11(4), 2010.

[37] Renée A Shellhaas and Robert R Clancy. Characterization of neonatal seizures by conventional EEG and single-channel EEG. *Clinical Neurophysiology*, 118(10):2156–2161, 2007.

[38] Nathan J Stevenson, Robert R Clancy, Sampsaa Vanhatalo, Ingmar Rosén, Janet M Rennie, and Geraldine B Boylan. Interobserver agreement for neonatal seizure detection using multichannel EEG. *Annals of clinical and translational neurology*, 2(11):1002–1011, 2015.

[39] Nathan J Stevenson, Leena Lauronen, and Sampsaa Vanhatalo. The effect of reducing EEG electrode number on the visual interpretation of the human expert for neonatal seizure detection. *Clinical Neurophysiology*, 129(1):265–270, 2018.

[40] Nathan J Stevenson, Karoliina Tapani, Leena Lauronen, and Sampsaa Vanhatalo. A dataset of neonatal EEG recordings with seizure annotations. *Scientific data*, 6:190039, 2019.

[41] Nathan J Stevenson, Karoliina Tapani, and Sampsaa Vanhatalo. Hybrid neonatal EEG seizure detection algorithms achieve the benchmark of visual interpretation of the human expert. In *2019 41st Annual International Conference of the IEEE Engineering in Medicine and Biology Society (EMBC)*, pages 5991–5994. IEEE, 2019.

[42] M Asjid Tanveer, Muhammad Jawad Khan, Hasan Sajid, and Noman Naseer. Convolutional neural networks ensemble model for neonatal seizure detection. *Journal of Neuroscience Methods*, 358:109197, 2021.

[43] Dapeng Tao, Jun Cheng, Zhengtao Yu, Kun Yue, and Lizhen Wang. Domain-weighted majority voting for crowdsourcing. *IEEE transactions on neural networks and learning systems*, 30(1):163–174, 2018.

[44] Karoliina T Tapani, Päivi Nevalainen, Sampsaa Vanhatalo, and Nathan J Stevenson. Validating an svm-based neonatal seizure detection algorithm for generalizability, non-inferiority and clinical efficacy. *arXiv preprint arXiv:2202.12023*, 2022.

[45] Hasan Tekgul, Blaise FD Bourgeois, Kimberlee Gauvreau, and Ann M Bergin. Electroencephalography in neonatal seizures: comparison of a reduced and a full 10/20 montage. *Pediatric neurology*, 32(3):155–161, 2005.

[46] Andriy Temko, Eoin Thomas, William Marnane, Gordon Lightbody, and Geraldine B Boylan. EEG-based neonatal seizure detection with support vector machines. *Clinical Neurophysiology*, 122(3):464–473, 2011.

[47] Andriy Temko, Eoin Thomas, William Marnane, Gordon Lightbody, and Geraldine B Boylan. Performance assessment for EEG-based neonatal seizure detectors. *Clinical Neurophysiology*, 122(3):474–482, 2011.

[48] Tian Tian and Jun Zhu. Max-margin majority voting for learning from crowds. In *Nips*, pages 1621–1629, 2015.

[49] Tammy N Tsuchida, Courtney J Wusthoff, Renée A Shellhaas, Nicholas S Abend, Cecil D Hahn, Joseph E Sullivan, Sylvie Nguyen, Steven Weinstein, Mark S Scher, James J Riviello, et al. American clinical neurophysiology society standardized EEG terminology and categorization for the description of continuous EEG monitoring in neonates: report of the American Clinical Neurophysiology Society critical care monitoring committee. *Journal of Clinical Neurophysiology*, 30(2):161–173, 2013.

[50] Anup Tuladhar, Sascha Gill, Zahinoor Ismail, Nils D Forkert, Alzheimer’s Disease Neuroimaging Initiative, et al. Building machine learning models without sharing patient data: A simulation-based analysis of distributed learning by ensembling. *Journal of biomedical informatics*, 106:103424, 2020.

[51] Lachlan Webb, Minna Kauppila, James A Roberts, Sampsaa Vanhatalo, and Nathan J Stevenson. Automated detection of artefacts in neonatal EEG with residual neural networks. *Computer Methods and Programs in Biomedicine*, 208:106194, 2021.

[52] David H Wolpert. Stacked generalization. *Neural networks*, 5(2):241–259, 1992.

[53] Nahathai Wongpakaran, Tinakon Wongpakaran, Danny Wedding, and Kilem L Gwet. A comparison of Cohen’s Kappa and Gwet’s AC1 when calculating inter-rater reliability coefficients: a study conducted with personality disorder samples. *BMC medical research methodology*, 13(1):1–7, 2013.

[54] Qiang Yang, Yang Liu, Yong Cheng, Yan Kang, Tianjian Chen, and Han Yu. Federated learning. *Synthesis Lectures on Artificial Intelligence and Machine Learning*, 13(3):1–207, 2019.

[55] Yuchen Zhang, Xi Chen, Dengyong Zhou, and Michael I Jordan. Spectral methods meet EM: A provably optimal algorithm for crowdsourcing. *The Journal of Machine Learning Research*, 17(1):3537–3580, 2016.

[56] Yuheng Zhang, Ruoxi Jia, Hengzhi Pei, Wenxiao Wang, Bo Li, and Dawn Song. The secret revealer: Generative model-inversion attacks against deep neural networks. In *Proceedings of the IEEE/CVF Conference on Computer Vision and Pattern Recognition*, pages 253–261, 2020.

Appendices

A Dawid–Skene method

The Dawid–Skene method was initially used to estimate the performance of human annotators [8]. Here the method is used to estimate the performance of models (local NSDAs) and obtain consensus judgement amongst them. The method is as follows. From a given set D of model predictions, the task is to estimate consensus labels $\{\mu_i\}_{i=1}^N$, the sensitivity α^j and specificity β^j of predictive model $j \in \{1, 2, \dots, R\}$. Let Y_e denote the multivariate random variable

$$Y_e = (Y_1^1, Y_1^2, \dots, Y_1^R, \dots, Y_N^1, Y_N^2, \dots, Y_N^R),$$

where random variable Y_i^j denotes the label given to instance i by model j . Furthermore, let T_i denote a random variable corresponding to the true label of instance i for which

$$P[T_i = 1] = t_i = t; \quad i \in \{1, 2, \dots, N\}.$$

Assuming that model labels are independent and that conditional probability of Y_i^j on T_i follows Bernoulli distribution with parameters α^j and β^j , respectively:

$$\begin{aligned} a_i &= P_\alpha [Y_i^1, Y_i^2, \dots, Y_i^R | T_i = 1] \\ &= \prod_{j=1}^R (\alpha^j)^{y_i^j} (1 - \alpha^j)^{1-y_i^j}; \quad i \in \{1, 2, \dots, N\}, \\ b_i &= P_\beta [Y_i^1, Y_i^2, \dots, Y_i^R | T_i = 0] \\ &= \prod_{j=1}^R (\beta^j)^{1-y_i^j} (1 - \beta^j)^{y_i^j}; \quad i \in \{1, 2, \dots, N\}. \end{aligned}$$

To simplify the notation, let $\theta = (t, \alpha, \beta)$ denote the parameters to be estimated. Assuming that instances are sampled independently, the likelihood function for Y_e is [8, 36]:

$$\begin{aligned} P_\theta[Y_e] &= \prod_{i=1}^N P_\theta[Y_i^1, Y_i^2, \dots, Y_i^R] \\ &= \prod_{i=1}^N \left(\underbrace{P_\theta[Y_i^1, Y_i^2, \dots, Y_i^R | T_i = 1]}_{a_i} \underbrace{P_\theta[T_i = 1]}_t \right. \\ &\quad \left. + \underbrace{P_\theta[Y_i^1, Y_i^2, \dots, Y_i^R | T_i = 0]}_{b_i} \underbrace{P_\theta[T_i = 0]}_{1-t} \right) \\ &= \prod_{i=1}^N (a_i t + b_i (1 - t)). \end{aligned} \tag{4}$$

Dawid and Skene used the EM algorithm to identify a local maximum of the likelihood function. The true labels are estimated by maximizing the likelihood function using estimated values for the sensitivity and specificity of each annotator, and the prior probability of class 1 (t), i.e. seizure. The algorithm has two main steps [8].

Expectation step: calculate the expected value of a true label knowing labels made by predictive models

$$\begin{aligned}
 \mu_i &= \mathbb{E}[T_i | Y_i^1, Y_i^2, \dots, Y_i^R] \\
 &= P_\theta[T_i = 1 | Y_i^1, Y_i^2, \dots, Y_i^R] \\
 &= \frac{P_\theta[Y_i^1, Y_i^2, \dots, Y_i^R | T_i = 1] P_\theta[T_i = 1]}{P_\theta[Y_i^1, Y_i^2, \dots, Y_i^R]} \quad (\text{Bayes' theorem}) \\
 &= \frac{a_i t}{a_i t + b_i (1 - t)}; \quad i \in \{1, 2, \dots, N\}.
 \end{aligned} \tag{5}$$

Maximization step: estimate t , α^j and β^j that maximize the likelihood function (4)

$$t = \frac{\sum_{i=1}^N \mu_i}{N}, \tag{6}$$

$$\alpha^j = \frac{\sum_{i=1}^N \mu_i y_i^j}{\sum_{i=1}^N \mu_i}; \quad j \in \{1, 2, \dots, R\}, \tag{7}$$

$$\beta^j = \frac{\sum_{i=1}^N (1 - \mu_i)(1 - y_i^j)}{\sum_{i=1}^N (1 - \mu_i)}; \quad j \in \{1, 2, \dots, R\}. \tag{8}$$

In the special case when all the μ_i 's are either 0 or 1, then t is the estimated ratio of positive instances and α^j (β^j) is an estimated ratio of correctly predicted positive (negative) examples by expert j , i.e. the estimated sensitivity (specificity) of expert j .

Input: $D, \epsilon = 10^{-5}, k_{max} = 5000$

Output: μ^{DS}

initialize $\mu^{DS} = \mu^M$

compute $\theta^{(0)}$ using equations (6), (7) and (8)

$k = 0$

repeat

$k = k + 1$

 compute μ^{DS} using equation (5)

 compute $\theta^{(k)}$ using equations (6), (7) and (8)

until $|\log P_{\theta^{(k-1)}}[Y_e] - \log P_{\theta^{(k)}}[Y_e]| < \epsilon$ **or** $k \geq k_{max}$

B Data information

Table 2: A summary of the data sets used in the study. Numbers inside parentheses represent standard deviation. Means for recordings are calculated across patients containing at least one consensus seizure longer than 16 sec (duration of one EEG segment).

	18-channel DS	3-channel DS
Number of patients	79	28
Number of patients with consensus seizures \geq 16 sec	38	24
Gestational age (weeks)	39.3 (2.1)	39.2 (2.0)
Number of derived EEG channels	18	3
Total recordings duration (hours)	111.9	2149.4
Mean recording duration (hours)	1.4 (0.6)	76.4 (35.8)
Total number of consensus seizures	344	1387
Total duration of consensus seizures (hours)	11.0	65.3
Mean duration of consensus seizures (minutes)	1.9 (2.7)	2.8 (6.0)
Mean fraction of recording containing seizures (%)	31.8 (26.4)	5.3 (5.6)
Mean fraction of recording containing consensus seizures (%)	19.1 (20.9)	3.5 (4.0)

C Architecture of the NSDA

In this work the NSDAs are deep neural networks consisted of three components, a feature extractor [29], an attention layer [19] and an output layer (figure 4). We used PyTorch implementation of layers for the feature extractor and for the output layer. Using PyTorch notation, the attention layer was implemented as follows. If an input to the attention layer is of size (N, C_{in}, L) then the output is of size (N, L) and can be described as

$$\text{out}(N_i) = \sum_{k=0}^{C_{in}-1} a_k \text{input}(N_i, k);$$

$$a_k = \frac{\exp(w^T \tanh(V\text{input}(N_i, k)^T))}{\sum_{j=0}^{C_{in}-1} \exp(w^T \tanh(V\text{input}(N_i, j)^T))},$$

where $V \in \mathbb{R}^{L \times \text{<inner size>}}$ and $w \in \mathbb{R}^{L \times 1}$ are learnable parameters.

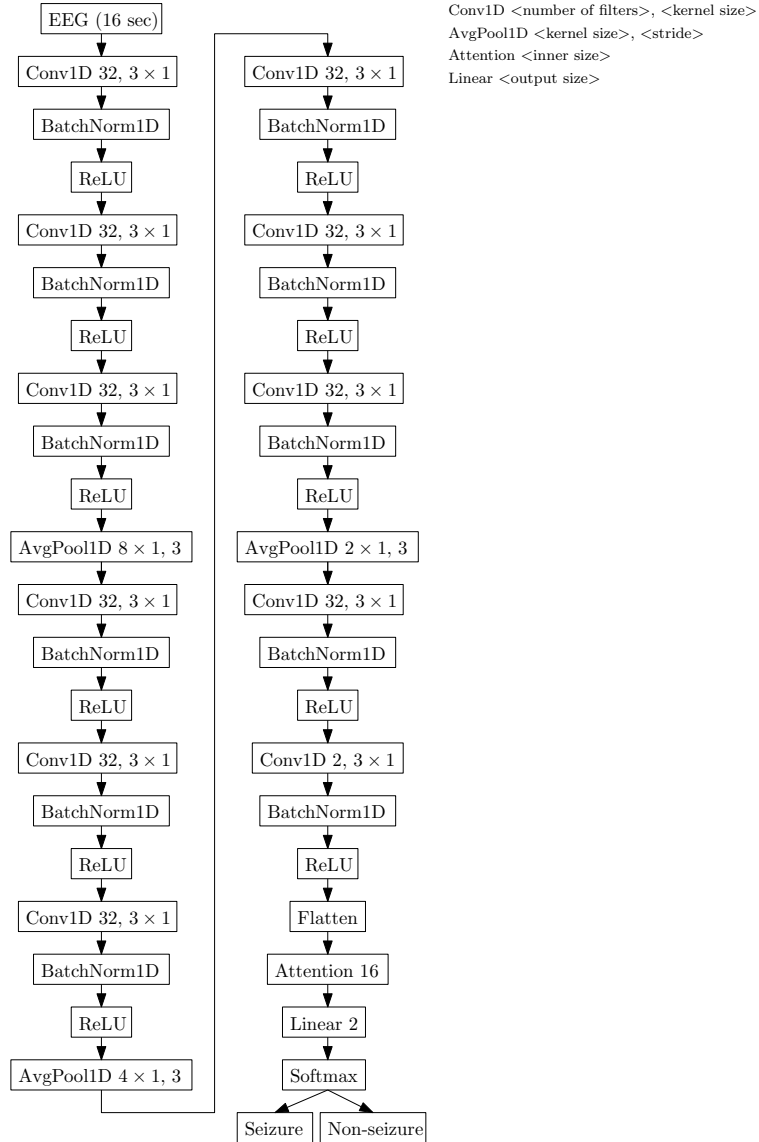


Figure 4: Architecture of the NSDA with a total of 29352 learnable parameters. Other parameters were set to default PyTorch values.

D Performance metrics

D.1 Segment-based metrics

Segment-based metrics were calculated based on 16 sec long EEG segments. A true positive (TP) is a correctly predicted seizure segment, a true negative (TN) is a correctly predicted non-seizure segment, a false positive (FP) is an incorrectly predicted non-seizure segment and a false negative (FN) is an incorrectly predicted seizure segment.

- Sensitivity (ratio of correctly predicted seizure intervals):

$$SE = \frac{TP}{TP + FN} \cdot 100.$$

- Specificity (ratio of correctly predicted non-seizure intervals):

$$SP = \frac{TN}{TN + FP} \cdot 100.$$

- Area under the receiver operating characteristics curve (AUC). The receiver operating characteristics curve describes SE depending on 1-SP.

D.2 Event-based metrics

Event-based metrics are in comparison with the segment-based metrics focused on each predicted seizure and not just 16 sec long segments. Three event-based metrics were used [47]:

- Seizure detection rate (SDR):

$$SDR = \frac{DS}{CS} \cdot 100,$$

where DS is a number of detected consensus seizures and CS is a number of consensus seizures. A seizure was considered to be detected if it was detected at any time of its duration.

- False detections per hour (FD/h):

$$FD/h = \frac{IDS}{D},$$

where IDS is a number of incorrectly detected seizures and D is duration of data in hours. A seizure was considered to be incorrectly detected if it is not overlapping with any seizure annotated by the experts.

- Mean false detection duration (MFDD):

$$MFDD = \begin{cases} 0; & \text{if } IDS = 0 \\ \frac{DIDS}{IDS}; & \text{otherwise} \end{cases},$$

where DIDS is a sum of durations of incorrectly detected seizures in seconds and IDS is a number of incorrectly detected seizures.

E Additional results

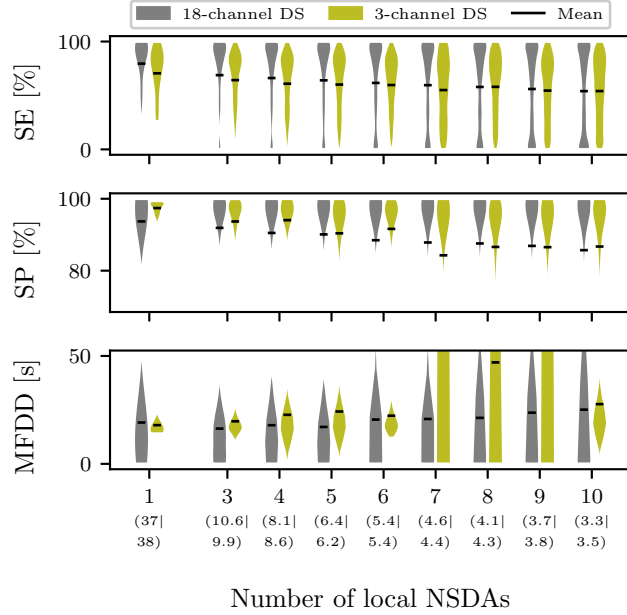


Figure 5: Performance of individual local NSDA. Sensitivity (SE), specificity (SP) and mean false detection duration (MFDD) of the local NSDAs as a function of the number of local NSDAs. The average (across ten runs) mean median number of patients in each NSDA is shown in parentheses. Each local NSDA was tested on a left-out patient from 18-channel DS or 3-channel DS.

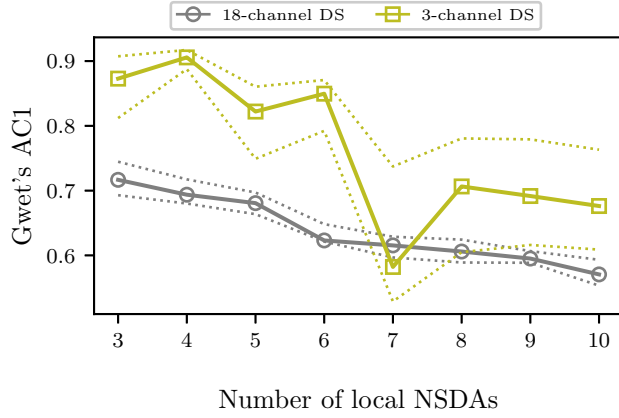


Figure 6: Average Gwet's AC1 between local NSDAs for 18-channel DS and 3-channel DS. The solid lines represent the medians of ten runs and dotted lines represent the corresponding inter-quartile ranges.

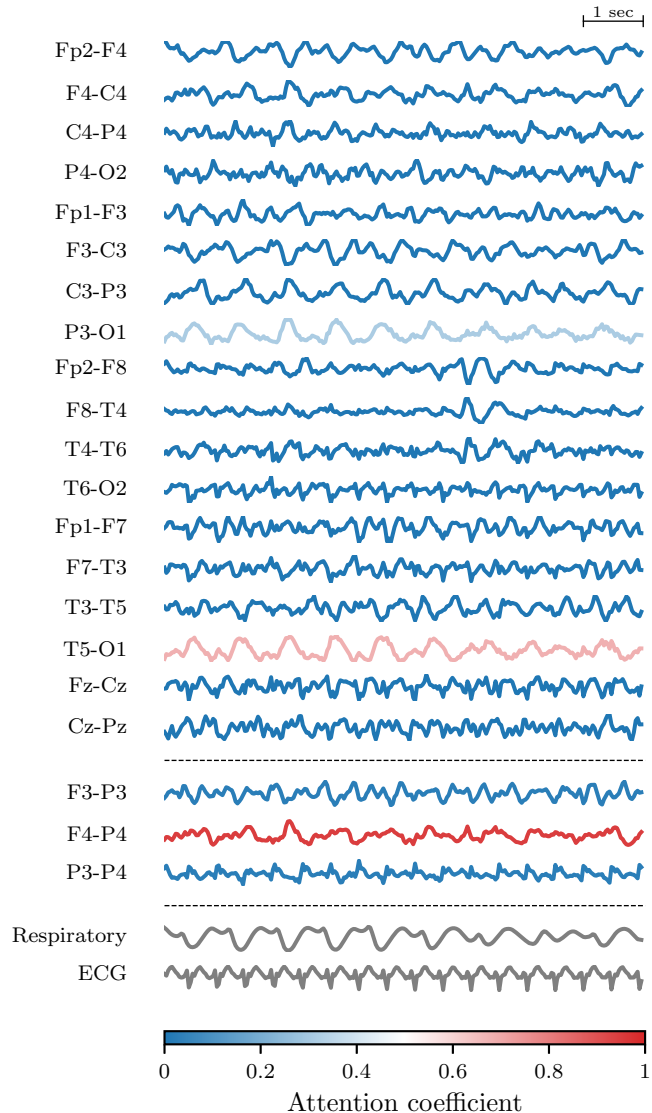


Figure 7: A half (8 sec) of a pre-processed EEG segment using 18-channel and 3-channel montages accompanied by the respiration and ECG at the bottom. The NSDA predicts a seizure when 18-channel montage is used and a non-seizure when 3-channel montage is used. Respiratory artefact is clearly visible on channels P3-01 and T5-O1 (attention coefficients are the largest for these two channels), the artefact is not visible in a 3-channel montage. Respiration and ECG signals were filtered and down-sampled as EEG signals were.

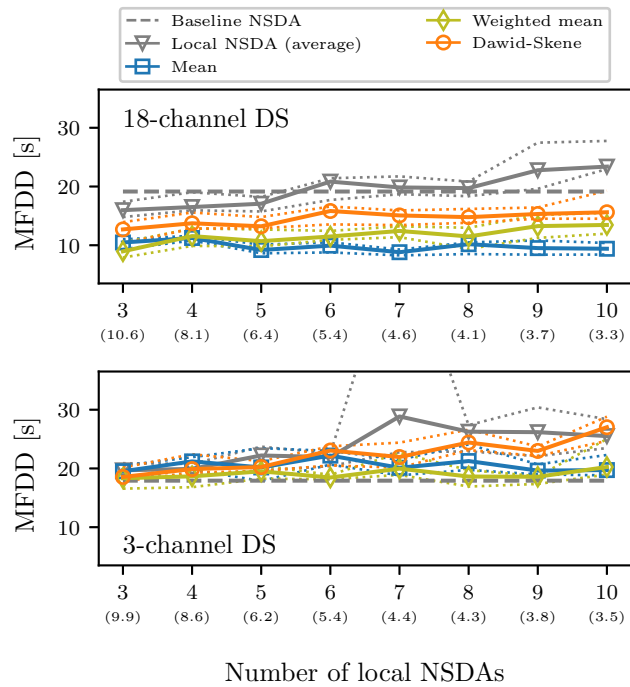


Figure 8: Average mean false detection duration (MFDD) as a function of the number of local NSDAs used in the aggregation schemes. The solid lines represent the medians of ten runs and dotted lines represent the corresponding inter-quartile ranges. The grey dashed line represents the average MFDD of the baseline NSDA.

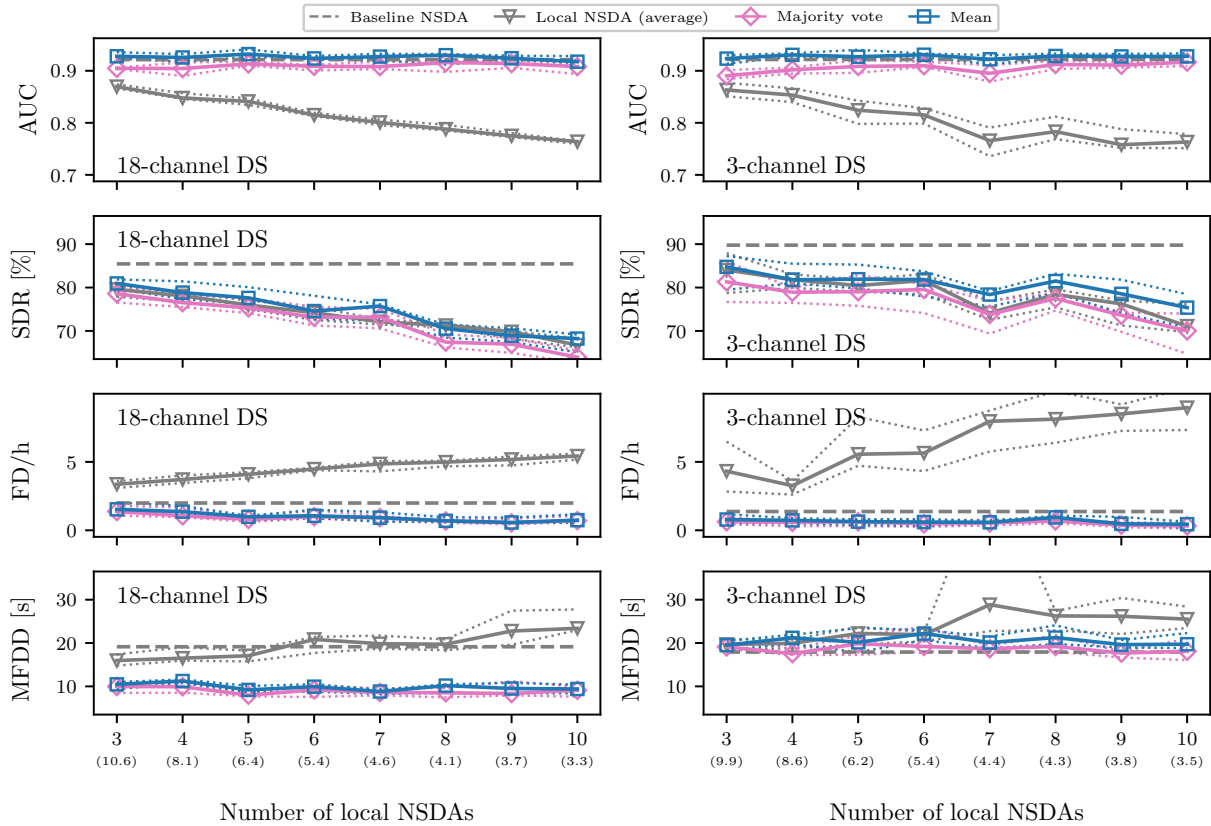


Figure 9: Average area under the curve (AUC), seizure detection rate (SDR), false detections per hour (FD/h) and false detection duration (MFDD) as a function of the number of local NSDAs used in the aggregation schemes. The solid lines represent the medians of ten runs and dotted lines represent the corresponding inter-quartile ranges. The grey dashed line represents the average metric of the baseline NSDA. The average (across ten runs) mean median number of patients in each NSDA is shown in parentheses.